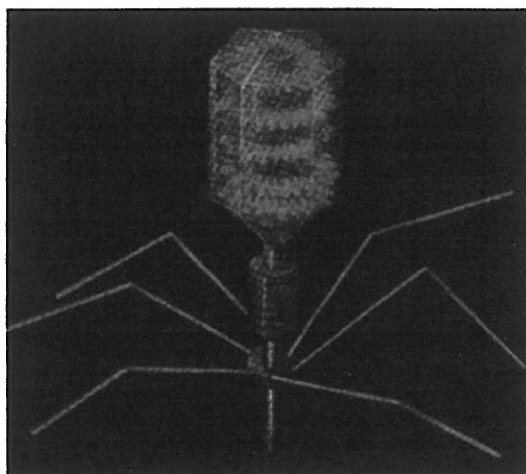
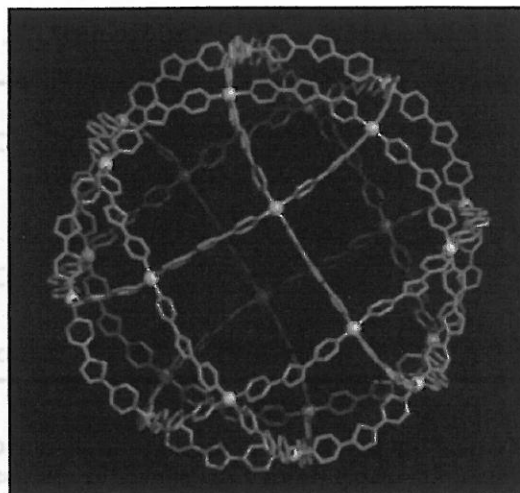


## Supramolecular Chemistry -Self-Assembled Complexes-



T4 Phage



The crystal structure of  $M_{24}L_{48}$   
( 24 palladium ions (M) and 48 curved bridging ligands (L))



**Makoto Fujita** received his PhD from the Tokyo Institute of Technology in 1987. Between 1988 and 1997 he worked as Assistant Professor, Lecturer, and then Associate Professor at Chiba University, 1997.1999 as Associate Professor at the Institute for Molecular Science (IMS) at Okazaki, and 1999.2002 as Full Professor at Nagoya University. In 2002 he became a Full Professor at The University of Tokyo. He has been a leader of the CREST project of the Japan Science and Technology Corporation since 1998. His research interests include metal-assembled complexes, molecular recognition, and nanometre-sized molecules.

---

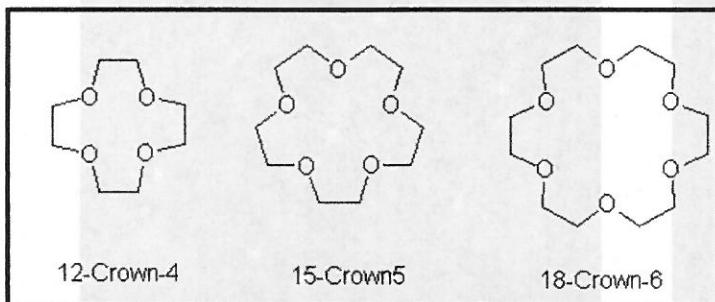
### Contents

- 0. Introduction
  - 1. Fujita work-Self-Assembled complexes-
    - 1-1. Metal-directed self-assembly of two- and three- dimensional synthetic receptor
      - 1-2. Self-Assembled  $M_{24}L_{48}$  Polyhedra
  - 2. Fujita work-Molecular Flasks-
    - 2-1. Diels-Alder reaction
    - 2-2. Photochemical Rearrangement and Radical Additions
    - 2-3. Catalyst
    - 2-4. Molecular Flasks as containers
  - 3. Summary and perspective
-

> Supramolecule

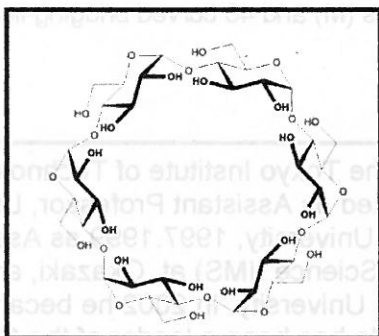
Supramolecule refers to compounds that some molecules are assembled by the noncovalent bonding interactions.

ex) C. J. Pedersen et al. *J. Am. Chem. Soc.* **1967**, *89*, 7017



Crown ether

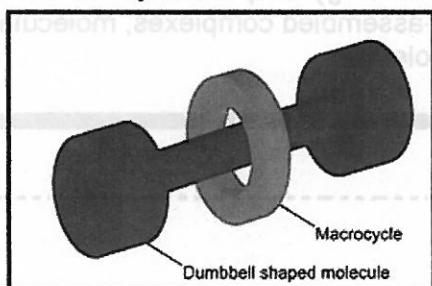
The denticity of the polyether influences the affinity of the crown ether for various cations. For example, 18-crown-6 has high affinity for potassium cation, 15-crown-5 for sodium cation, and 12-crown-4 for lithium cation.



Cyclodextrin

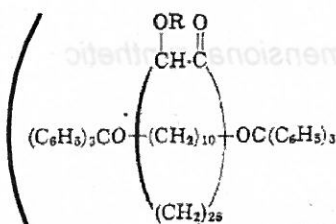
Cyclodextrins formed stable aqueous complexes with many other chemicals.

The formation of the inclusion compounds greatly modifies the physical and chemical properties of the guest molecule, mostly in terms of water solubility.



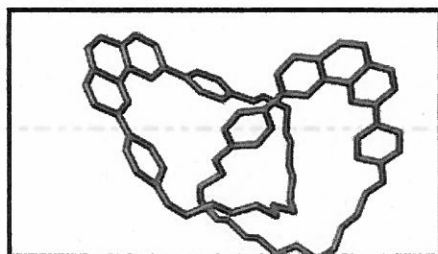
Rotaxane

A rotaxane is a mechanically-interlocked molecular architecture consisting of a "dumbbell shaped molecule" which is threaded through a "macrocycle".

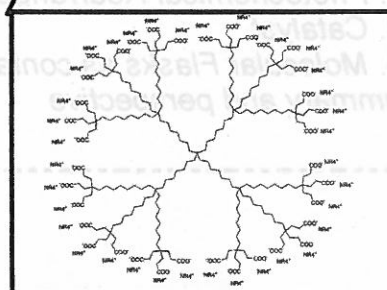


example of rotaxane  
*J. Am. Chem. Soc.* **1967**, *89*, 5723.

2, R = H  
6, R = CO(CH<sub>2</sub>)<sub>2</sub>CO<sub>2</sub> resin



catenane

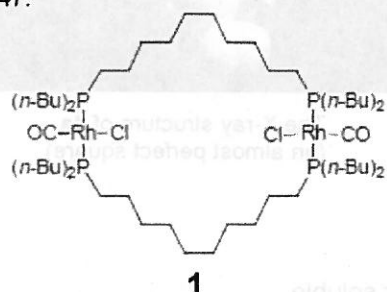


Dendrimer

## 1-1. Metal-directed self-assembly of two- and three- dimensional synthetic receptor

> An earlier example of metal-ligand macrocycles was the macrocyclic dinuclear Rh(I) complex 1.

A. J. Pryde, B. L. Shaw and B. Weeks, *J. Chem. Soc., Chem. Commun.*, 1973, 947.

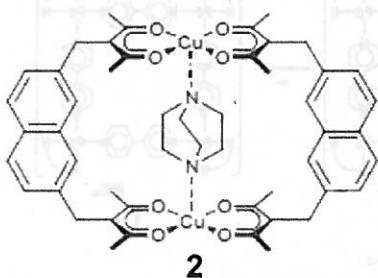


1

However, it was not designed as a receptor and no binding property was reported for this or related macrocycles.

> The first self-assembled macrocyclic host 2 containing two Cu(II) ions

A. W. Maverick and F. E. Klavetter, *Inorg. Chem.*, 1984, 23, 4129.



2

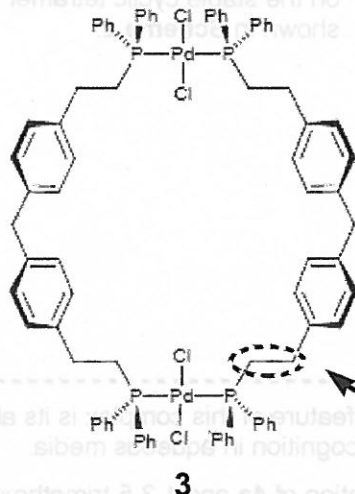
This macrocycle showed a strong binding affinity towards 1,4-diazabicyclo[2.2.2]octane ( $K_a = 220 \text{ L mol}^{-1}$ ) as evidenced by X-ray crystallography. Two point acid-base binding observed in the crystal structure is obviously important because little affinity was shown for monoamines such as pyridine ( $K_a = 0.5 \text{ L mol}^{-1}$ ).

Table 1 Association constants between self-assembled macrocycles and various guests

Host	Guest	Association constant/L mol <sup>-1</sup>
2	Pyridine	0.5
	Pyradine	5
	Quinuclidine	7
	DABCO	220

> Macrocyclic dinuclear Pd(II) complex 3 has a hydrophobic cavity.

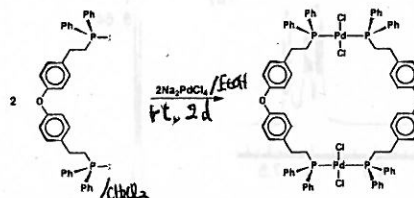
M. Fujita, J. Yazaki, T. Kuramochi and K. Ogura, *Bull. Chem. Soc. Jpn.*, 1993, 66, 1837.



3

(Spontaneous self-assembly process)

Scheme 1



The  $-\text{CH}_2\text{CH}_2-$  units reduce the steric repulsion among the aromatic rings after cyclization, which otherwise prevents the assembling of the macrocycle.

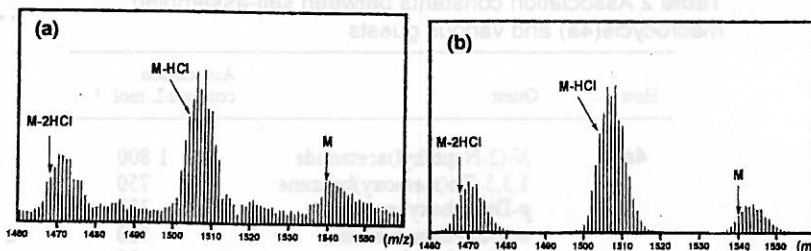
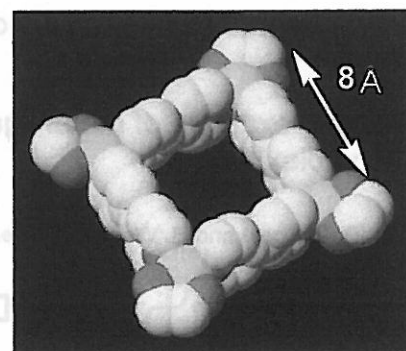
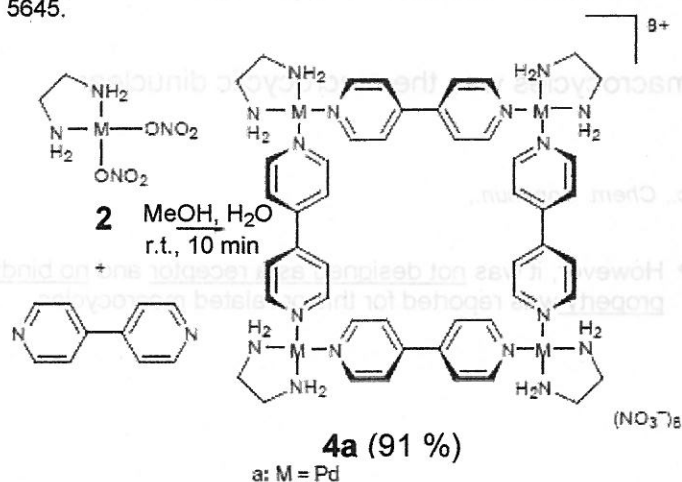


Figure 1 FAB MS of 3 : (a) found (b) distributions for M, M-HCl, and M-2HCl fragments.

> The first example of the self-assembled complex possessing cisprotected Pd(II) blocks is the tetranuclear square compound **4a**.

No.4

M. Fujita, J. Yazaki and K. Ogura, *J. Am. Chem. Soc.*, 1990, 112, 5645.



The X-ray structure of **4a**  
(an almost perfect square)

Due to the cationic structure, complex **4a** is highly water soluble.

Scheme 2

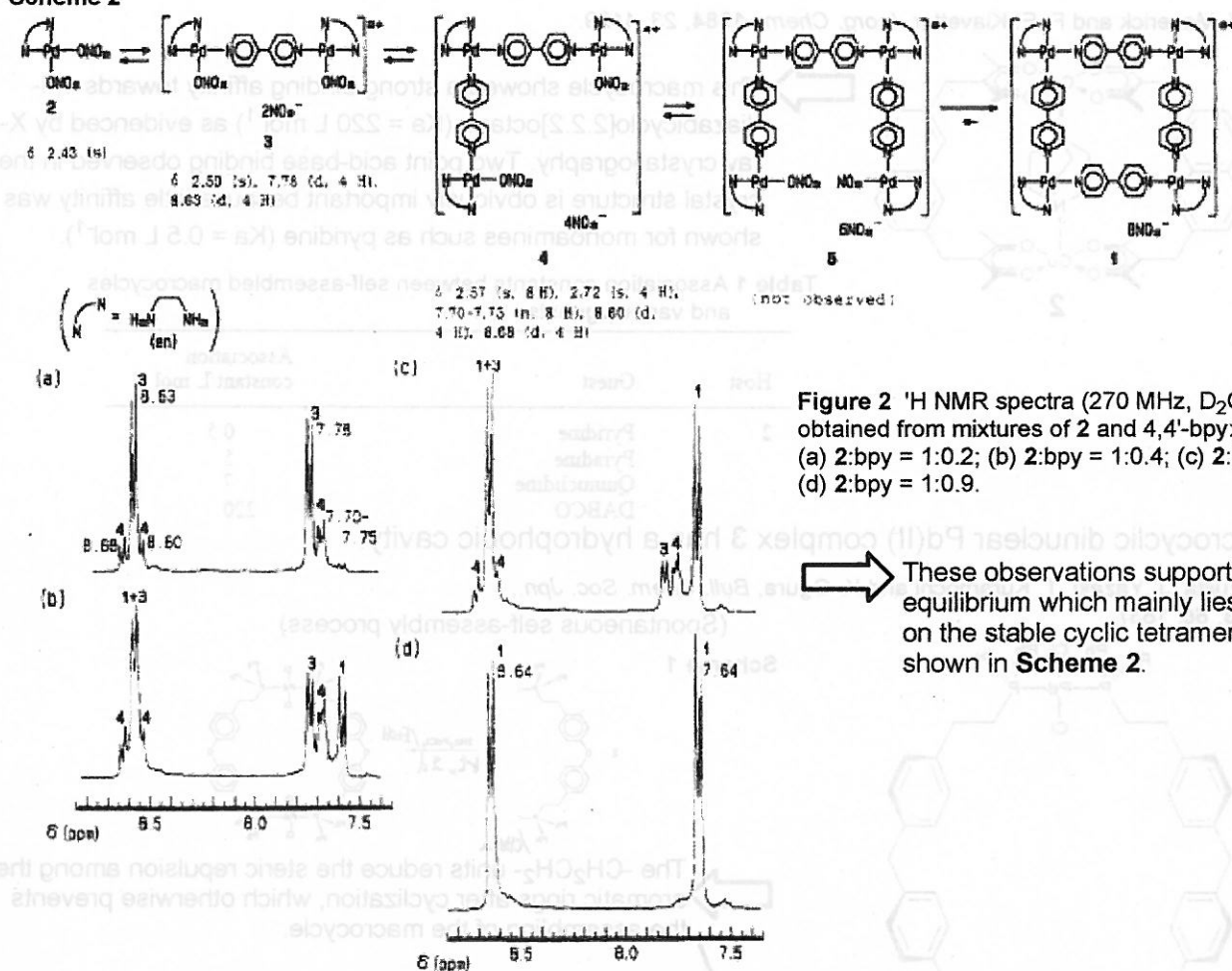


Figure 2 <sup>1</sup>H NMR spectra (270 MHz, D<sub>2</sub>O) obtained from mixtures of **2** and 4,4'-bpy: (a) 2:bpy = 1:0.2; (b) 2:bpy = 1:0.4; (c) 2:bpy = 1:0.6; (d) 2:bpy = 1:0.9.

These observations support rapid equilibrium which mainly lies on the stable cyclic tetramer **1** (**4a**) as shown in Scheme 2.

Table 2 Association constants from self-assembled macrocycle(**4a**) and various guests

Host	Guest	Association constant/L mol <sup>-1</sup>
<b>4a</b>	<i>N</i> -(2-Naphthyl)acetamide	1 800
	1,3,5-Tri(methoxy)benzene	750
	<i>p</i> -Dimethoxybenzene	330
	<i>m</i> -Dimethoxybenzene	580
	<i>o</i> -Dimethoxybenzene	30
	<i>p</i> -Bis(methoxymethyl)benzene	10
	1,4-(Dimethoxy)cyclohexane	n.c. <sup>a</sup>

<sup>a</sup>n.c.: not complexed.

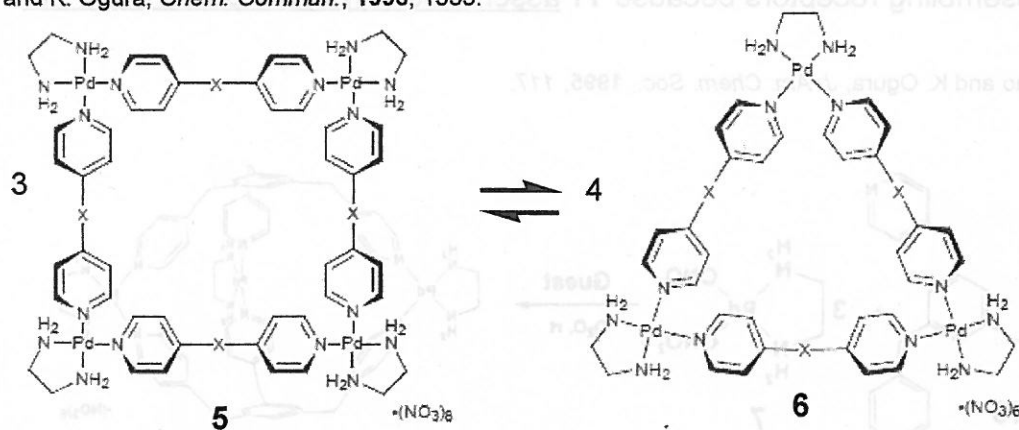
A significant feature of this complex is its ability for molecular recognition in aqueous media.

The complexation of **4a** and 1,3,5-trimethoxybenzene is 1 : 1 and the association constant (*K*<sub>a</sub>) at 25 °C is 7.5 × 10<sup>2</sup> L mol<sup>-1</sup>.

> The square structure was easily expanded by incorporating phenylene or acetylene spacers into the bipyridine framework.

No.5

M. Fujita, O. Sasaki, T. Mitsuhashi, T. Fujita, J. Yazaki, K. Yamaguchi and K. Ogura, *Chem. Commun.*, 1996, 1535.



a: X =  $-\text{C}\equiv\text{C}-$ ; b: X =  $-\text{CH}=\text{CH}-$ ; c: X =  $-\text{C}\equiv\text{C}-\text{C}\equiv\text{C}-$ ; d: X =  $-\text{C}_6\text{H}_4-$

However, an equilibrium between square **5** and triangle **6** was observed depending on the concentration of the components.

> The treatment of tripyridyl compound **8** with **7** gave nano-sized macrotricyclic complex **9**.

M. Fujita, S-Y. Yu, T. Kusakawa, H. Funaki, K. Ogura and K. Yamaguchi, *Angew. Chem., Int. Ed. Engl.*, 1998, 37, in the press.

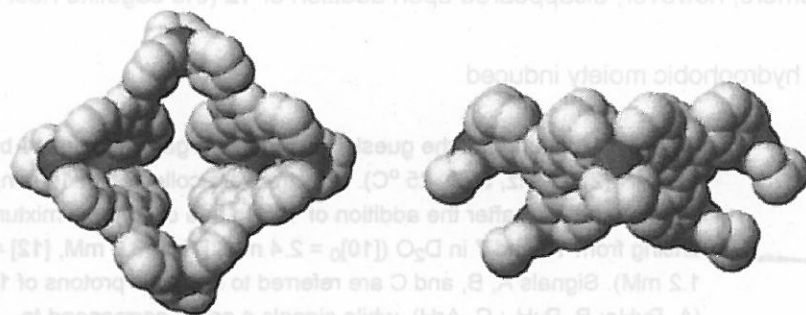
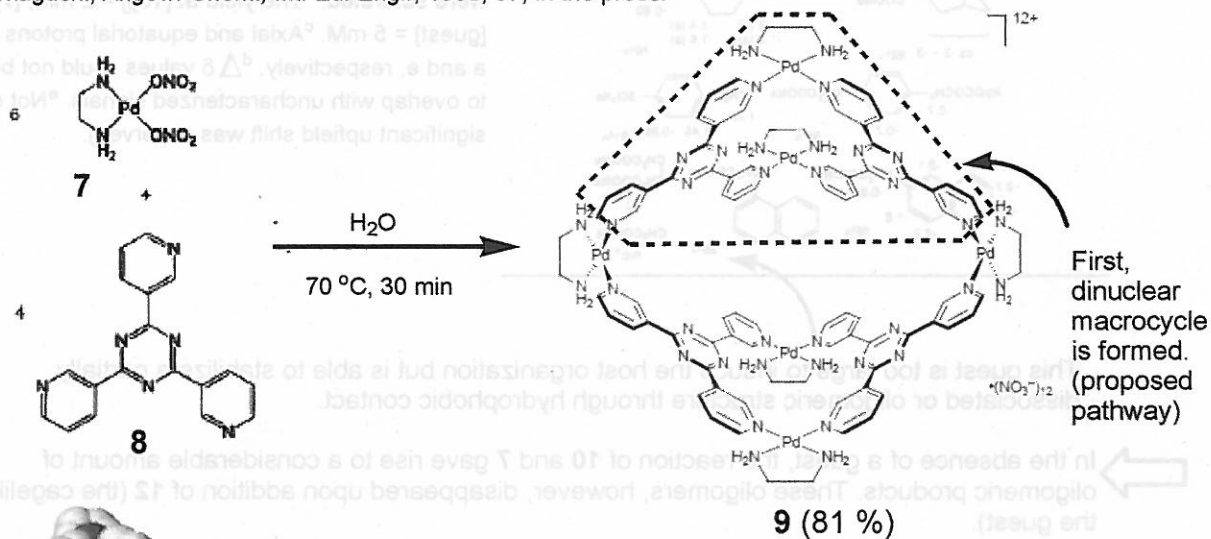


Figure 3 X-ray structure of **9**. Left: a top view; right: a side view.

The structure of **9** was determined by X-ray crystallographic analyses.

The open cavity of **9** is surrounded by 16 aromatic rings and thus is hydrophobic, whereas the outside surface is hydrophilic due to the exposure of six charged Pd(II) centers.

> A cage-like complex is compound **11** assembled from three molecules of **7** and two simple, pyridine-based ligands **10**. The behavior of this complex is quite different from that of other self-assembling receptors because **11** assembles only in the presence of an appropriate guest.

M. Fujita, S. Nagao and K. Ogura, *J. Am. Chem. Soc.*, 1995, 117, 1649.

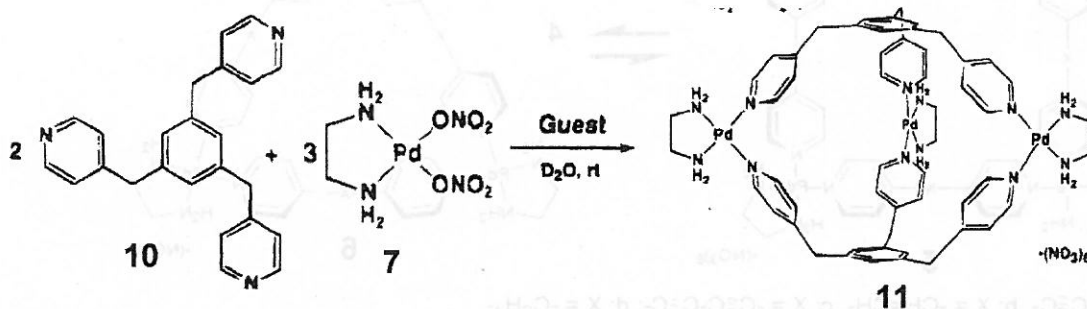
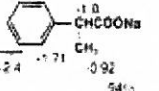
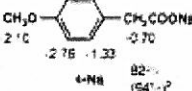
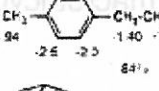
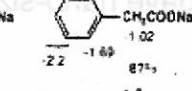
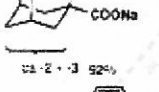
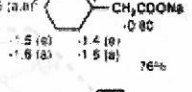
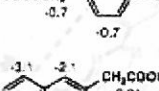
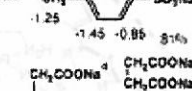
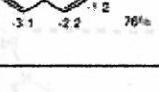
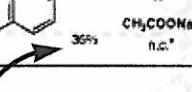


Table 3 Guest-Induced Organization of **11**

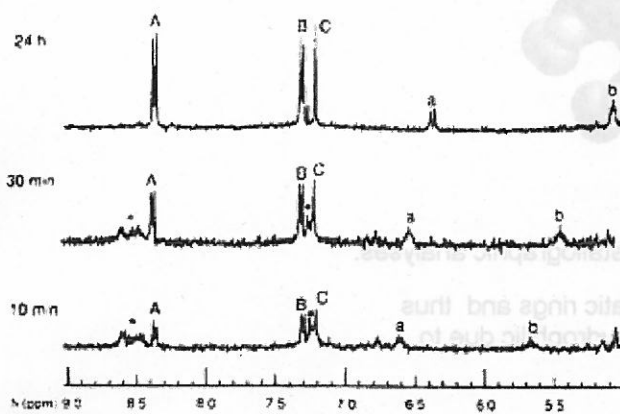
	
	
	
	
	

<sup>a</sup>The NMR yield of **11** is determined at  $[10]_0 = 2$  mM,  $[7]_0 = 3$  mM, and  $[guest] = 1.5$  mM unless otherwise noted and is shown below each structure. The negative values shown with each structure present upfield shift ( $\Delta\delta$  in ppm) in <sup>1</sup>H NMR measured at  $[10]_0 = 6$  mM,  $[7]_0 = 9$  mM, and  $[guest] = 1.5$  mM. At these conditions, titration experiments showed that the  $\Delta\delta$  values of the guests (except  $C_6H_4(COONa)_2$ ) were saturated. <sup>b</sup>The yield at  $[10]_0 = 2$  mM,  $[7]_0 = 3$  mM, and  $[guest] = 5$  mM. <sup>c</sup>Axial and equatorial protons are donated by a and e, respectively. <sup>d</sup> $\Delta\delta$  values could not be analyzed due to overlap with uncharacterized signals. <sup>e</sup>Not complexed (no significant upfield shift was observed).

This guest is too large to induce the host organization but is able to stabilize a partially dissociated or oligomeric structure through hydrophobic contact.

➡ In the absence of a guest, the reaction of **10** and **7** gave rise to a considerable amount of oligomeric products. These oligomers, however, disappeared upon addition of **12** (the cage-like host binds the guest).

➡ Various anionic guests having a hydrophobic moiety induced the organization of **11** (Table 3).



**Figure 4** Monitoring of the guest-induced self-organization of **11** by <sup>1</sup>H NMR (270 MHz,  $D_2O$ , 25 °C). Spectra were collected at 10 min, 30 min, and 24 h after the addition of **12**·Na to a oligomeric mixture arising from **10** and **7** in  $D_2O$  ( $[10]_0 = 2.4$  mM,  $[7]_0 = 3.6$  mM,  $[12] = 1.2$  mM). Signals A, B, and C are referred to aromatic protons of **11** (A, PyHa; B, PyHg; C, ArH), while signals a and b correspond to aromatic protons of **12**. The signal b at 24 h is overlapping with a side band of  $H_2O$  signal. Complicated signals appearing at  $\delta$  7.1-7.3 and 8.4-8.7 (indicated by asterisks) are attributed to oligomeric components. ArCH<sub>2</sub> signals of **11** appeared as a singlet ( $\delta$  3.97), showing that twisting of the three-dimensional framework of **11** is rapid on the NMR time scale. A singlet signal at  $\delta$  7.3 is referred to  $CHCl_3$ , slightly contained in the external TMS/ $CDCl_3$  solution.

### > Self-Assembled $M_{24}L_{48}$ Polyhedra and Their Sharp Structural Switch upon Subtle Ligand Variation



The structure of the multicomponent system is highly sensitive to the geometry of the bent ligands. Even a slight change in the ligand bend angle critically switches the final structure observed across the entire ensemble of building blocks between  $M_{24}L_{48}$  and  $M_{12}L_{24}$  coordination spheres. The amplification of this small initial difference into an incommensurable difference in the resultant structures is a key mark of emergent behavior.

M. Fujita et al., *SCIENCE*, 2010, 328,1144

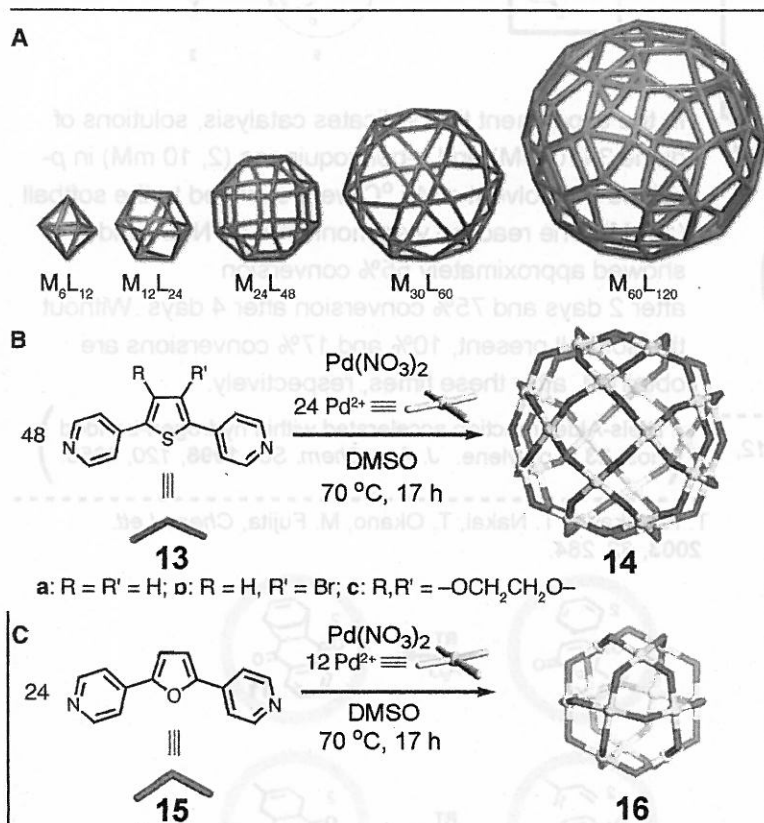
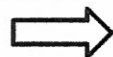


**Figure 5** (A) The family of  $MnL_{2n}$  polyhedra where metals (M) and bridging ligands (L) are mapped onto the vertices and edges, respectively, of the polyhedra. (B) Self-assembly of  $M_{24}L_{48}$  spheres **14**. (C) Self-assembly of  $M_{12}L_{24}$  sphere **16**.



In terms of enthalpy, ligand **13** should favor assembly into a less-distorted rhombicuboctahedron, whereas ligand **15** should lie on the midline between angles favoring a cuboctahedron versus a rhombicuboctahedron. The selective formation of  $M_{12}L_{24}$  from ligand **15** is rationalized by reduced loss of entropy for  $M_{12}L_{24}$  than for  $M_{24}L_{48}$  (which incorporates more components). If ligand **13** were to form a  $M_{12}L_{24}$  cuboctahedron, substantial pinching and distortion would offset the entropic advantage; thus the enthalpically favored  $M_{24}L_{48}$  forms instead.

the slight difference in ligand bend angle  $149^\circ$  in **13** and  $127^\circ$  in **15**, based on a density functional theory (DFT) calculation



The ratio of ligand **13c** and **15** was then varied sequentially from 9:1 to 1:9, and, surprisingly, only pure  $M_{12}L_{24}$  or  $M_{24}L_{48}$  was observed (**Table 4**). Starting from 100% of ligand **1**,  $M_{24}L_{48}$  assembled exclusively until the ratio of **13c:15** was 2:8.

**Table 4** Self-organization criticality of **13c** and **15** mixtures.

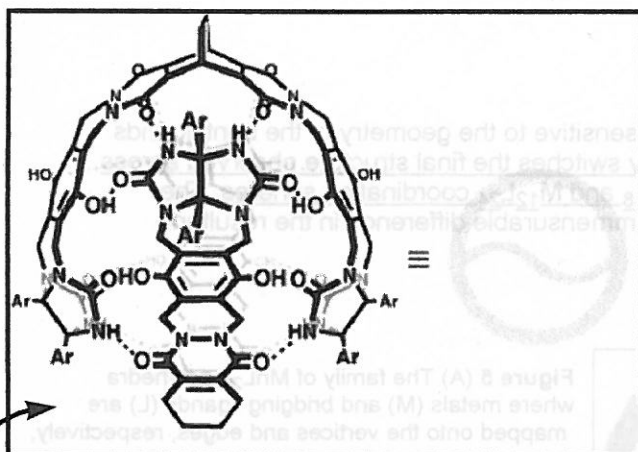
13c:15 ratio (angle)*	Product
10:0 (149.3)	$M_{24}L_{48}$ only
9:1 (147.1)	$M_{24}L_{48}$ only
8:2 (144.8)	$M_{24}L_{48}$ only
7:3 (142.6)	$M_{24}L_{48}$ only
6:4 (140.3)	$M_{24}L_{48}$ only
5:5 (138.1)	$M_{24}L_{48}$ only
4:6 (135.9)	$M_{24}L_{48}$ only
3:7 (133.6)	$M_{24}L_{48}$ only
2:8 (131.4)	$M_{12}L_{24}$ only
1:9 (129.1)	$M_{12}L_{24}$ only
0:10 (126.9)	$M_{12}L_{24}$ only

\*Mean bent angle ( $^\circ$ ).

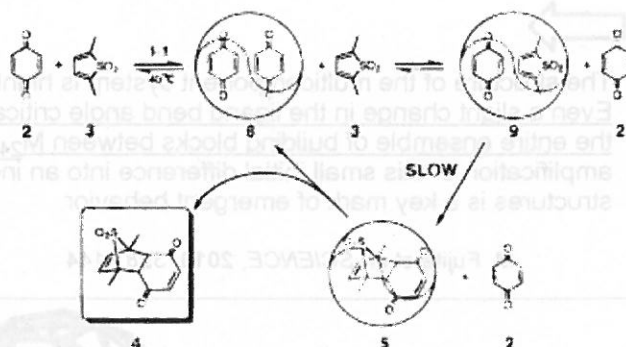
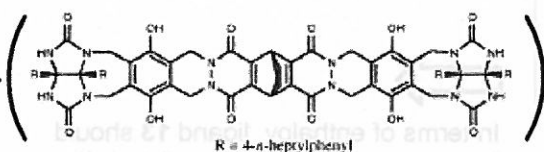
## 2-1. Diels-Alder reaction

R. Wyler, J. de Mendoza, J. Rebek, Jr., *Angew. Chem. Int. Ed. Engl.* **1993**, *32*, 1699.*J. Am. Chem. Soc.* **1998**, *120*, 1389.

(The proposed catalytic cycle)

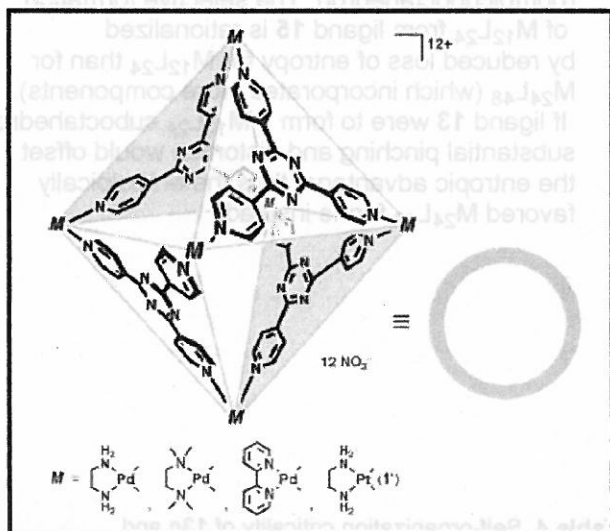


The hydrogen-bonding "softball" capsule 17 dimer



In the experiment that indicates catalysis, solutions of diene 3 (10 mM) and *p*-benzoquinone (2, 10 mM) in *p*-xylene- $d_{10}$  solvent at 40 °C were exposed to the softball (1 mM). The reaction was monitored by NMR and showed approximately 55% conversion after 2 days and 75% conversion after 4 days. Without the softball present, 10% and 17% conversions are obtained, after these times, respectively.

(Diels-Alder reaction accelerated within hydrogen-bonded host 23 in *p*-xylene. *J. Am. Chem. Soc.* **1998**, *120*, 3650.)

M. Fujita, J. Yazaki, K. Ogura, *J. Am. Chem. Soc.* **1990**, *112*, 5645.

The self-assembled octahedral cage 18

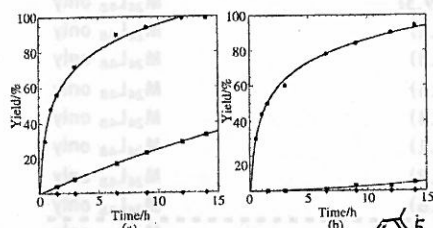
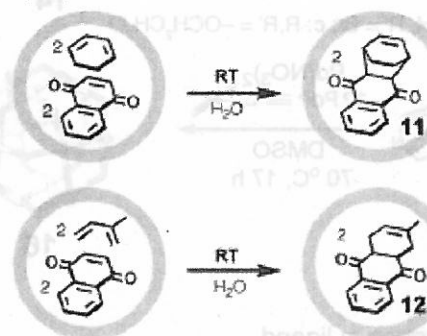


Figure 17 Time course of the Diels-Alder reactions of 2 with dienes 3 (a) and 5 (b) at 25 °C. (●): in the presence of 1 in water, (■): in the absence of 1 in water. (◆): control experiment in  $CHCl_3$ .

T. Kusakawa, T. Nakai, T. Okano, M. Fujita, *Chem. Lett.* **2003**, *32*, 284.

Diels-Alder reactions accelerated within 18 which binds large molecules in aqueous media.

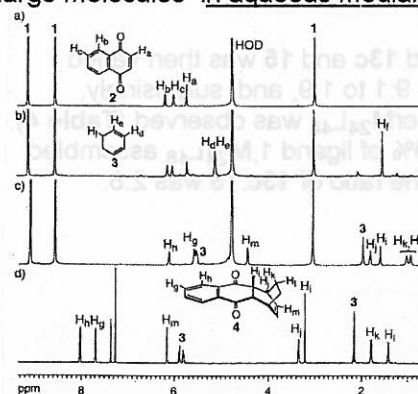


Figure 6  $^1H$  NMR monitoring of the  $D_2O$  phase in the Diels-Alder reaction of 1,4-naphthoquinone (2) and 1,3-cyclohexadiene (3). (a) Only 2 equiv. of naphthoquinone was enclathrated in the cavity of 1. (b) 10 equiv. (vs 1) of 1,3-cyclohexadiene was added to the solution. (c) After stirred at 25 °C for 24 h. (d) After being extracted with  $CDCl_3$ , was identified as Diels-Alder adduct 4.

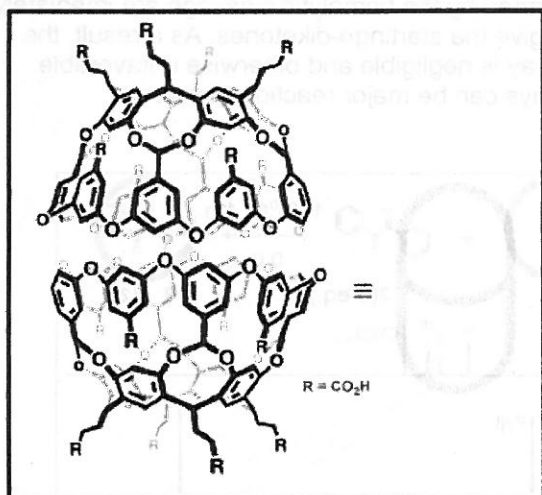


## 2-2. Photochemical Rearrangements and Radical Additions

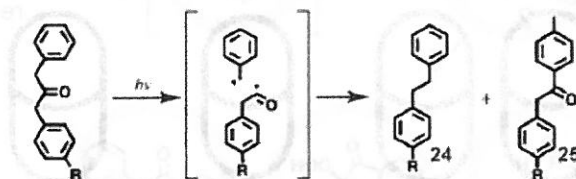
C. L. D. Gibb, B. C. Gibb, *J. Am. Chem. Soc.* **2004**, *126*, 11408.

L. S. Kaanumalle, C. L. D. Gibb, B. C. Gibb, V. Ramamurthy, *J. Am. Chem. Soc.* **2004**, *126*, 14366.

C. L. D. Gibb, A. K. Sundaresan, V. Ramamurthy, B. C. Gibb, *J. Am. Chem. Soc.* **2008**, *130*, 4069-5080.



The hydrophobic dimeric capsule **19**



Unusual photochemical rearrangements of dibenzyl ketones within hydrophobic capsule **19** in an aqueous buffer. Norrish type I.

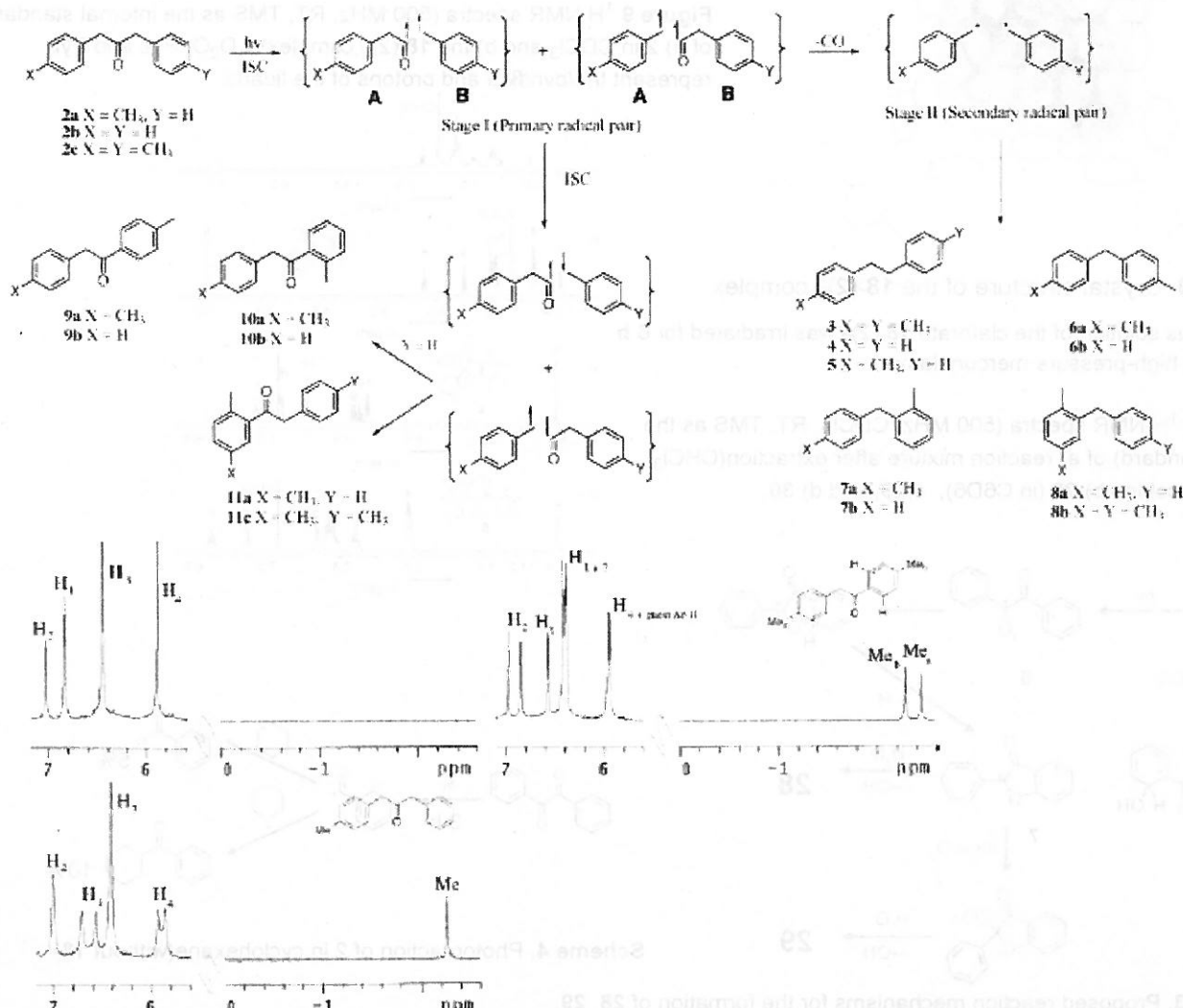


**Figure 8** Selected regions of the  $^1\text{H}$  NMR of: (left top) host **19** (see structure for designations), (left bottom) the capsular complex **19**<sub>2a</sub>, (right top) the capsular complex **19**<sub>9a</sub>. Host concentration ) 1 mM; guest concentration ) 0.5 mM.

Further addition of guests results in  $^1\text{H}$  NMR peaks corresponding to free guest.

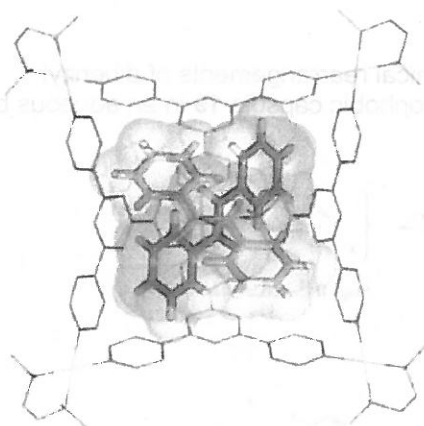
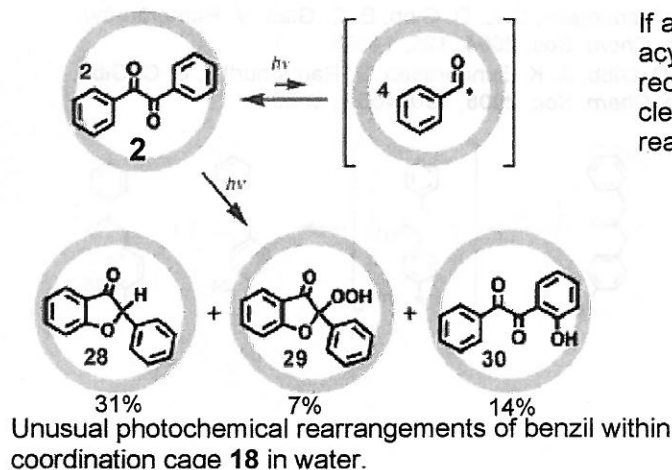
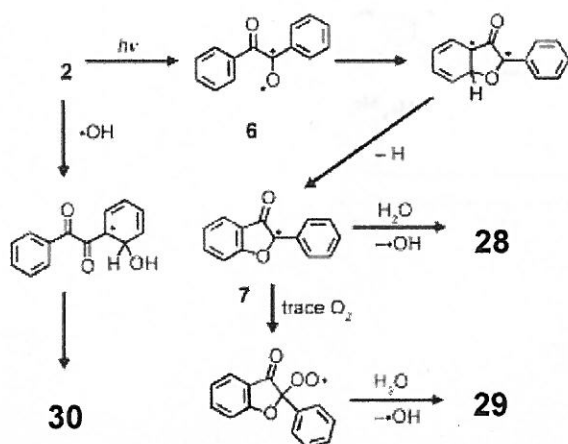


**Figure 10.** Crystal structure of the **18(2)<sub>2</sub>** complex.

An aqueous solution of the clathrate **18(2)<sub>2</sub>** was irradiated for 6 h by using a high-pressure mercury lamp.

**Figure 11.** <sup>1</sup>H NMR spectra (500 MHz, CDCl<sub>3</sub>, RT, TMS as the internal standard) of a) reaction mixture after extraction (CHCl<sub>3</sub>), purified by column b) **28** (in C<sub>6</sub>D<sub>6</sub>), c) **29**, and d) **30**.



**Scheme 3.** Proposed reaction mechanisms for the formation of **28**, **29**, and **30**.

If adiketones are confined in a restricted cavity of cages, the acyl radicals formed by the homolytic cleavage are immediately recombined to give the starting  $\alpha$ -diketones. As a result, the cleavage pathway is negligible and otherwise unfavorable reaction pathways can be major reaction courses.

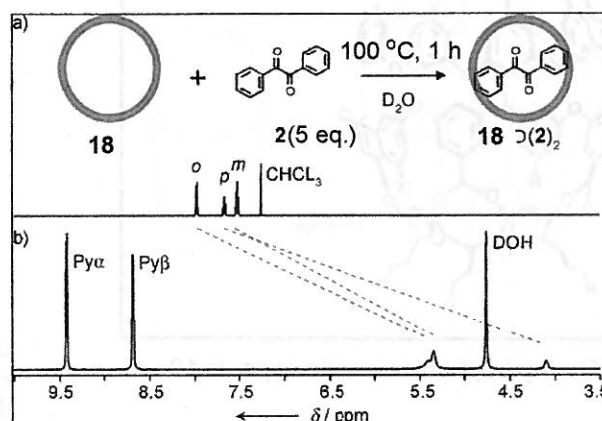
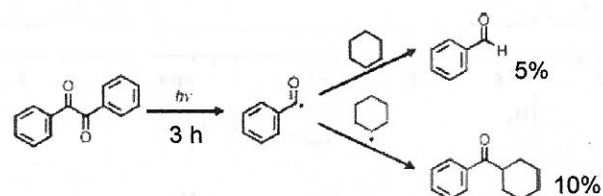
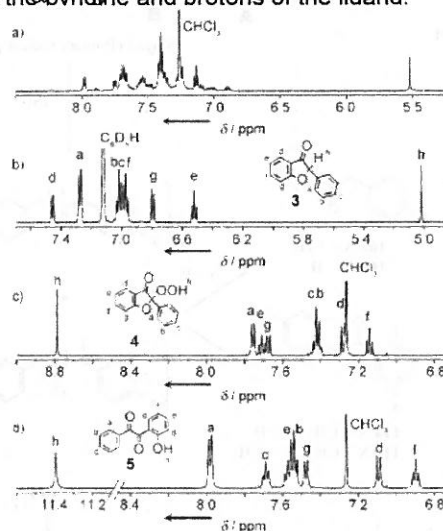
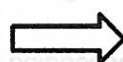


**Figure 9** <sup>1</sup>H NMR spectra (500 MHz, RT, TMS as the internal standard) of a) **2** in CDCl<sub>3</sub> and b) the **18(2)<sub>2</sub>** complex in D<sub>2</sub>O. Py $\alpha$  and Py $\beta$  represent the  $\alpha$ -protons and protons of the ligand.



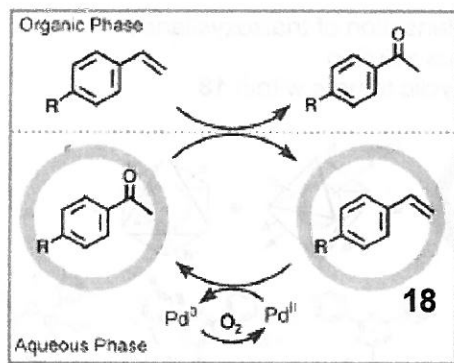
**Scheme 4.** Photoreaction of **2** in cyclohexane (without **18**).



They emphasize that the diketone homolytic cleavage is completely suppressed within cage **18** and that kinetically unfavorable pathways without homolytic cleavage became major pathways thanks to the remarkable cage effect of **18**.

## 2-3. Catalyst

H. Ito, T. Kusakawa, M. Fujita, *Chem. Lett.* **2000**, 598.

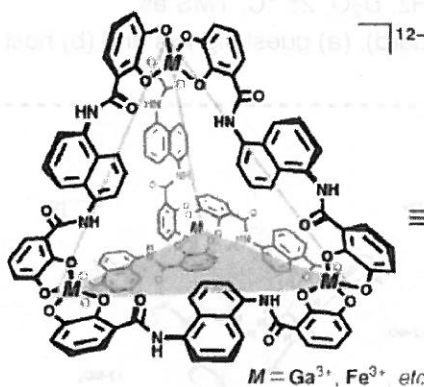


Wacker-type oxidation of styrenes in the presence of **18** and [(en)Pd(NO<sub>3</sub>)<sub>2</sub>].

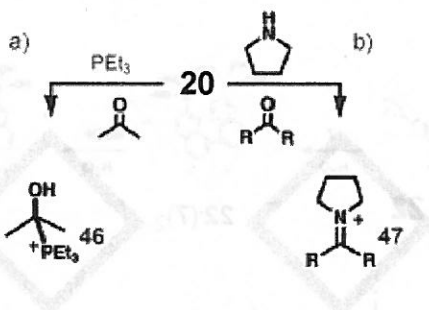
Due to the strong binding ability of **18** toward electron-rich aromatic compounds, the reaction was particularly efficient for electron-rich substrates. The reaction was also sensitive to the size of the substrates.

## 2-4. Molecular Flasks as Containers

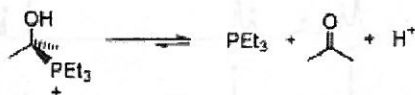
D. L. Caulder, R. E. Powers, T. N. Parac, K. N. Raymond, *Angew. Chem. Int. Ed.* **1998**, 37, 1840.



Tetrahedral coordination capsule **20**



Stabilization of a) phosphonium ions and b) iminium ions within **20** in water.



Scheme 6 Decomposition of **46** in water

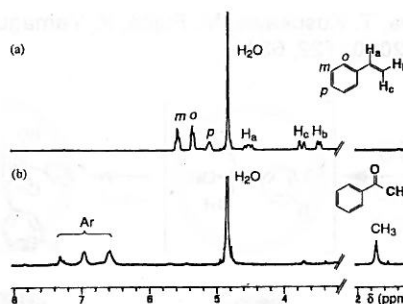


Figure 12. <sup>1</sup>H NMR monitoring of the D<sub>2</sub>O phase in the aerobic oxidation of styrene catalyzed by **18** and (en)Pd(NO<sub>3</sub>)<sub>2</sub>. (a) Only styrene was treated with the D<sub>2</sub>O solution of **18**. (b) (en)Pd(NO<sub>3</sub>)<sub>2</sub> was added and the D<sub>2</sub>O phase was monitored after 24 h at 80 °C.

Table 5. Aerobic oxidation of styrene and its derivatives catalyzed by **18** and 2[(en)Pd(NO<sub>3</sub>)<sub>2</sub>].

Run	Ar	<b>18</b> / mol%	2 / mol%	Yield of ketones / % <sup>b</sup>
1	phenyl	10	10	82
2	phenyl	-	10	4
3 <sup>a</sup>	phenyl	10	10	3
4	phenyl	10	-	4
5	<i>p</i> -methoxyphenyl	10	10	53
6	<i>p</i> -tolyl	10	10	64
7	<i>p</i> -nitrophenyl	10	10	13
8	2-naphthyl	10	10	12

<sup>a</sup>1,3,5-Trimethoxybenzene (1 equiv to styrene) was added.  
<sup>b</sup>Determined by <sup>1</sup>H NMR.

M. Ziegler, J. L. Brumaghim, K. N. Raymond, *Angew. Chem. Int. Ed.* **2000**, 39, 4119.

V. M. Dong, D. Fiedler, B. Carl, R. G. Bergman, K. N. Raymond, *J. Am. Chem. Soc.* **2006**, 128, 14464.

## Scheme 5 Stabilization of Iminium Ions in Aqueous Solution by Molecular Encapsulation

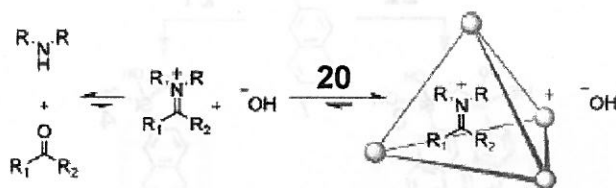
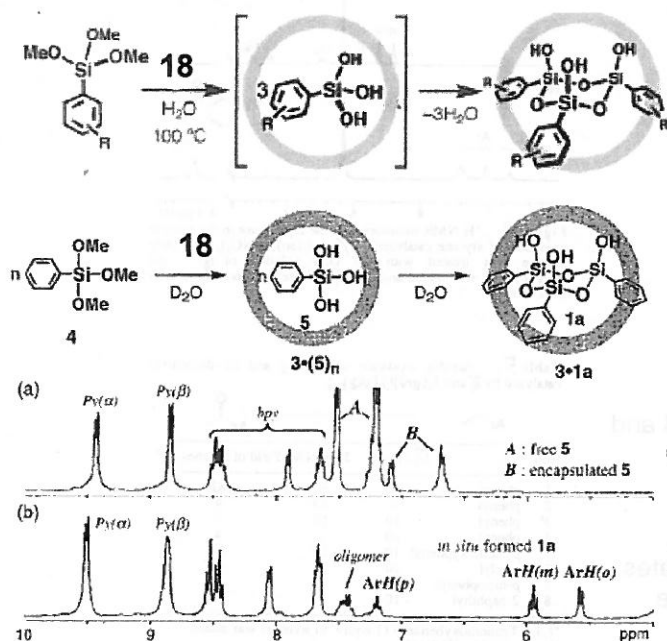


Table 6 Molecular Recognition of Iminium Ions Generated in Water from Pyrrolidine and Various Ketones

entry	ketone	R	n	product	binding efficiency <sup>a</sup> (%)
1	acetone	Me	0	2	63
2	2-butanone	Me	1	3	66
3	2-pentanone	Me	2	4	82
4	2-hexanone	Me	3	5	80
5	2-heptanone	Me	4	6	68
6	2-octanone	Me	5	7	67
7	2-nonanone	Me	6	8	28
8	2-undecanone	Me	7	9	0
9	3-pentanone	Et	2	10	85
10	3-hexanone	Et	3	11	90
11	3-heptanone	Et	4	12	66
12	3-octanone	Et	5	13	32
13	3-nonanone	Et	6	14	0



**Figure 13** Monitoring of the condensation of **4** to **1a** in nanocage **18** by  $^1\text{H}$  NMR (300 MHz,  $\text{D}_2\text{O}$ , 25 °C, TMS as an external standard): (a) after 5 min at 100 °C and (b) after 1 h at 100 °C.

M. Yoshizawa, T. Kusakawa, S. Sakamoto, K. Yamaguchi, *J. Am. Chem. Soc.* **2001**, *123*, 10454.

M. Aoyagi, K. Biradha, M. Fujita, *J. Am. Chem. Soc.* **1999**, *121*, 7457.

Polycondensation of trialkoxysilanes in aqueous solution to form cyclic trimers within **18**.

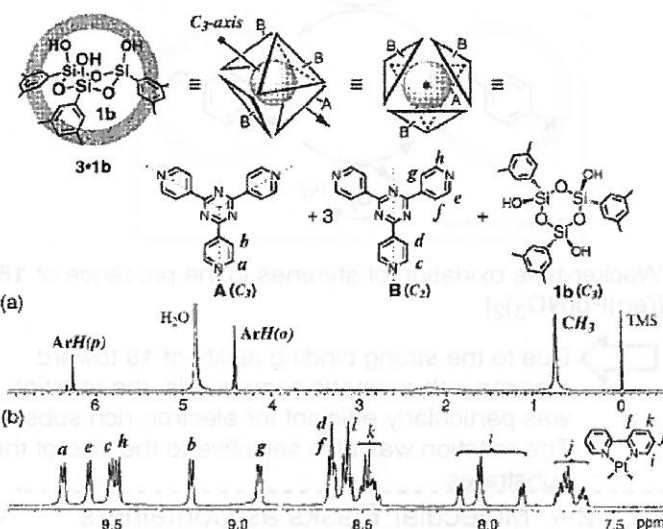
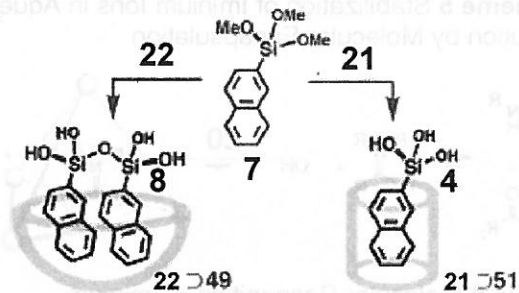


**Figure 14** Schematic representation of the  $\text{C}_3$ -symmetric structure of **18 1b** and the  $^1\text{H}$  NMR spectrum of **18 1b** (500 MHz,  $\text{D}_2\text{O}$ , 25 °C, TMS as an external standard): (a) guest signals and (b) host signals.



Isolation of specific intermediates in the polycondensation of trialkoxysilanes within **22** and **21** in water.

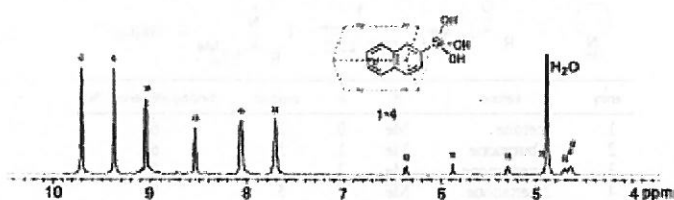
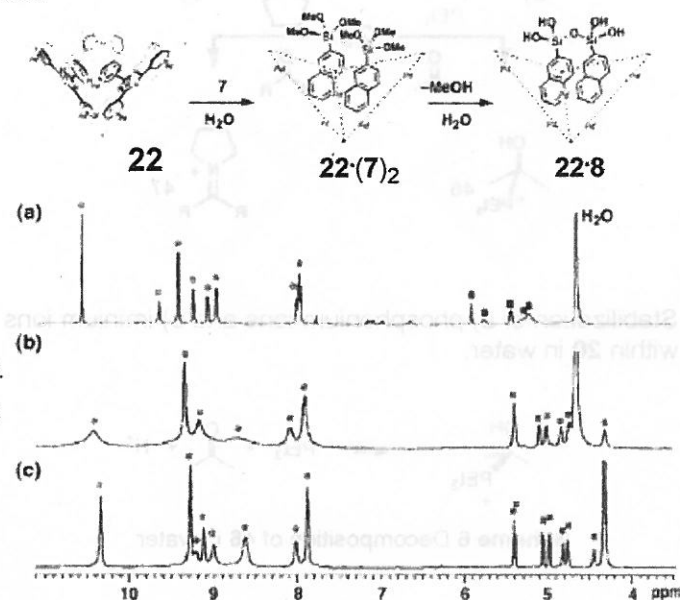
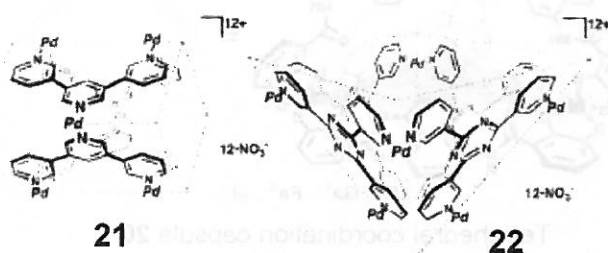


**Figure 15**  $^1\text{H}$  NMR spectrum (500 MHz,  $\text{D}_2\text{O}$ , TMS as an external standard) of **21•4** at 27 °C. Circles and squares indicate host and guest signals, respectively.

**Figure 16**  $^1\text{H}$  NMR spectrum (500 MHz,  $\text{D}_2\text{O}$ , TMS as an external standard) of (a) **22•(7)<sub>2</sub>** at 27 °C and variable-temperature  $^1\text{H}$  NMR spectrum of **22•8** at (b) 27 and (c) 60 °C. Circles and squares indicate host and guest signals, respectively.



### 3. Summary and Perspective

>Fujita demonstrated the effectiveness of the metalmediated self-assembly strategy for constructing two- and three-dimensional receptor frameworks and self-assembled molecular flasks.

These strategies provides the facile preparation of synthetic receptors and, more significantly, enables the construction of nanosized, precise structures never before prepared by conventional covalent synthesis.

A more important aspect in this area is that the self-assembled complexes may exhibit new and unexpected properties particularly owing to the binding abilities of the receptor frameworks and the redox or magnetic properties of the metals.

The metal directed self-assembly complexes will bring a variety of applications to current chemistry which have never been achieved by covalent bond chemistry.